

Short Communication

## Analysis on the Corrosion Performance of Friction Stir Welding Joint of 7022 Aluminum Alloy

Hong-feng Wang<sup>1,2</sup>, Jian-li Wang<sup>1</sup>, Wei-wei Song<sup>1</sup>, Dun-wen Zuo<sup>2</sup>, Ding-lin Shao<sup>2</sup>

<sup>1</sup> College of Mechanical and Electrical Engineering, Huangshan University, Huangshan 245041, P.R.China;

<sup>2</sup> College of Mechanical and Electrical Engineering, Nanjing University of Aeronautics and Astronautics, Nanjing 210016, P.R.China)

\*E-mail: [jnjllhy@163.com](mailto:jnjllhy@163.com)

Received: 22 March 2016 / Accepted: 23 May 2016 / Published: 7 July 2016

---

The corrosion performances of base metal (i.e. 7022 aluminum alloy) and the welded joints under different process parameters of 7022 aluminum alloy in the mixed solution of Na<sub>2</sub>SO<sub>4</sub> + dilute H<sub>2</sub>SO<sub>4</sub> (pH = 5) were studied by the weight-loss method and electrochemical method. The weight-loss method results showed that the base metal and the welded joints under different process parameters were occurred corrosion on their surfaces, and the base metal corrosion was far greater than the welded joints under different process parameters, the parameter for 400 /30 welded joint corrosion was minimum. The electrochemical corrosion results were consistent with weight-loss method. Under various parameters of welded joints corrosion rate were not consistent, the parameters for 400 /30 welded joint corrosion rate was lowest. The electrochemical corrosion results showed that the base metal corrosion was mainly for pitting and denser distribution. The welded joints under different process parameters corrosion were appeared only a small amount of spot, their corrosion degree were small.

---

**Keywords:** friction stir welding; 7022 aluminum alloy; corrosion performance; electrochemical method; weight-loss method

### 1. INTRODUCTION

With the development of aircraft manufacturing industry, the manufactures of the large aircraft structures have been shifted from the traditional melt riveting and welding to friction stir welding (FSW) applied widely. FSW is a solid-state method of joining thermoplastic materials, in which rotating tool is inserted into the adjoining edges of the sheets to be welded with a proper tilt angle and moved all along the joint. The Tool rotation and welding speeds will lead to the surface between the

tool and the base metal to flow, and under the action of extrusion of the tool, the welding seam is formed. Recently, FSW is the major aircraft manufacturing enterprises due to the reduction of the molten defects in the welded joints and the improvement of the welding quality [1-3]. Aircraft operation environment is bad, especially the international long distance transport aircraft. The aircraft always fly in the changing environment, sometimes in the harsh environment. The corrosion has a great impact on the plane because of long exposure in the atmosphere. As the aircraft structures, the corrosion resistance of aluminum alloy becomes one of the hottest researches [4-7]. Yong et al. [8] studied the stress corrosion behavior of friction stir welding joint using slow strain tensile and electrochemical corrosion of 7A52 aluminum alloy, and find out that impressed cathodic polarization increases the stress corrosion index of 7A52 aluminum alloy. Zhang et al. [9] studied the corrosion properties of the welded joints of 2219 aluminum alloy in 3.5% NaCl solution, and pointed out that the corrosion resistance of the friction stir welding joint is superior to those of other fusion welding joints. Lu et al. [10] prepared a layer of micro-arc oxidation film on the surface of friction stir welding joints in 5083 aluminum alloy, showed that the micro-arc oxide film layer could improve the corrosion resistance of joint. Ji et al. [11] investigated the corrosion resistance of friction stir welding joints of 5383 aluminium alloy, showed that the corrosion resistance welded joint S line is the worst. Hu et al. [12] studied the corrosion resistance of friction stir welding joint of LY12 aluminum alloy in 3.5% NaCl solution, and find out that the corrosion resistance of the heat affected zone is the worst, the corrosion resistance of heat-affected zone is the best. Dong et al. [13] studied the corrosion resistance of friction stir welded joint of 2A12 aluminum alloy coated with aluminum layer in the solution of 0.2 mol/L NaHSO<sub>3</sub> + 0.6 mol/L NaCl at room temperature, and pointed out that the package aluminum layer can effectively protect the corrosion of welding joint. Kang et al. [14] pointed out that high rotation speed can improve the microstructure and corrosion resistance of welded joints of 2024 aluminum alloy. The corrosion behaviors of friction stir welding joints of AA2219 aluminum alloy and 2195 aluminum alloy are also investigated by Surekha et al. [15] and Omar et al. [16]. Recently, 7022 aluminum alloy has attracted more interests due to its higher tensile strength and yield strength, excellent wear and corrosion resistance, good performance of friction stir welding. However, there is less work on the properties of the welded joints of 7022 aluminum alloy. This determines the 7022 aluminum alloy instead of 7075 and 7050 aluminum alloy also need quite a long time. Only more mastery of 7022 aluminum alloy friction stir welding properties, it can be gotten better application. Therefore, this paper is to study the corrosion resistance of the welded joints of 7022 aluminum alloy, to explore the corrosion mechanism of the welded joints. It can provide theoretical support for 7022 aluminum alloy FSW joints application under the corrosive environment, and strive for the early realization of 7022 aluminum alloy instead of 7075 and 7050 aluminum alloy.

## 2. EXPERIMENTAL PROCEDURES

### 2.1 Material preparation

Two 7022 aluminum alloy plates with the size of 200×100×10mm was used for FSW. FSW has two important parameters: the rotation speed and the welding speed of the tool. FSW was carried out at

the rotation speed of 300, 400 and 600 rpm for a single-pass employing a welding speed of 30, 50 and 100 mm/min and tool tilt angle of 2.5°. The depth of processing was kept as 1.7 mm. In the present paper, the samples were denoted as X/Y. The X and Y are respectively the rotation speed and the welding speed. Table 1 shows the serial number of the experimental alloys.

**Table 1.** The sample number of the experimental alloys.

Sample number	Base metal	1	2	3	4	5	6	7	8	9
X(rpm)	0	300	300	300	400	400	400	600	600	600
Y (mm/min)	0	30	50	100	30	50	100	30	50	100

### 2.2 Corrosion characterization

The corrosion samples with the size of 15×15×5 mm were machined in the transverse direction from the nugget zone. Corrosion behavior of the welded joints was investigated using corrosion immersion tests and electrochemical corrosion study. All samples were ground with SiC emery papers of up to 2000 grit and finely polished with 0.5µm diamond powder, and then ultrasonically cleaned in alcohol for 5 min and dried in air. Then the sample was immersed in the mixed solution of Na<sub>2</sub>SO<sub>4</sub> + dilute H<sub>2</sub>SO<sub>4</sub> (pH=5) at the ambient temperature (25 °C). These solutions were prepared with A. R. grade chemicals and distilled water. The weight measurement was conducted with Sartorius BP121S electro-optical analytical balance after removing corrosion products from the surface of specimens.

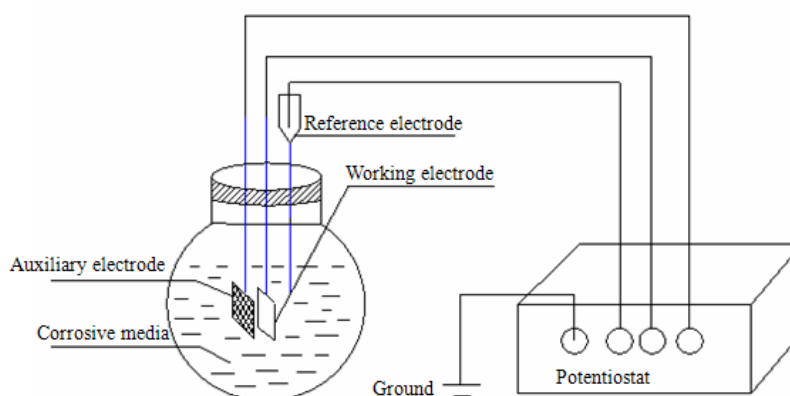


**Figure 1.** Schematic diagram of electrochemical experimental installation.

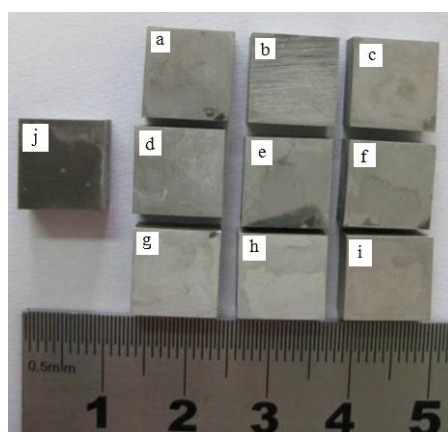
Electrochemical tests were carried out on a CHI660C electrochemical workstation as shown in Fig.1. A three-electrode cell with the sample as the working electrode (exposed area of 1 cm<sup>2</sup>), saturated calomel electrode (SCE) as the reference electrode and platinum plate as the counter electrode was used. First, the samples were sealed by AB glue, exposed an area of 1 cm<sup>2</sup>. Second, the

samples were cleaned by acetone, ethyl alcohol and distilled water, respectively. Third, the samples were immersed in the solution for 5 min. Finally, the polarisation tests were carried out between scanning potentials from -2.0 V to 1.0 V relative to the open circuit potential (OCP) at a scan rate of 0.01 V/s, similar to the works in Refs.17 and 18. Scanning electron microscopy (SEM, S-4800) were used to observe the morphology and probe the chemical compositions of the welded joints before and after the corrosion tests.

### 3. RESULTS AND DISCUSSION

#### 3.1 Weight loss measurements

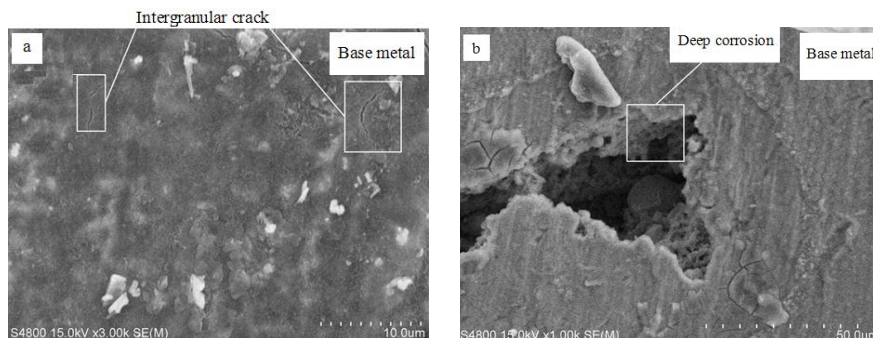
Fig. 2 shows the corrosion surface images of 7022 aluminum alloy (the base metal) and welded joints of 7022 aluminum alloy under different process parameters after immersion in the corrosion solution. It can be observed that the parent metal exhibits poor corrosion resistance, the whole surface of the sample is covered by the black corrosion products. Meanwhile, the corrosion areas of the welding joints under different process parameters show a large variation. The samples 1, 3, 6 and 7 exhibit small black area with the size of 2~4 mm<sup>2</sup>, the color change of the corrosion surface in samples 2 and 5 is large, and the size of corrosion area is about 10mm<sup>2</sup>. The samples 4, 8 and 9 show a lighter color. It can be concluded that the corrosion resistance of the welding joints is better than the base metal. The grain size of the base metal is inhomogeneous, which results in more dislocation defects during rolling process. While, the uniform equiaxed grains can be obtained in the welding joints through the dynamic recrystallization of the grain size due to the strong mechanical and thermal effect caused by the stirring processing, which can reduces defects significantly. Therefore, the corrosion resistance of the welding joints can be improved effectively.



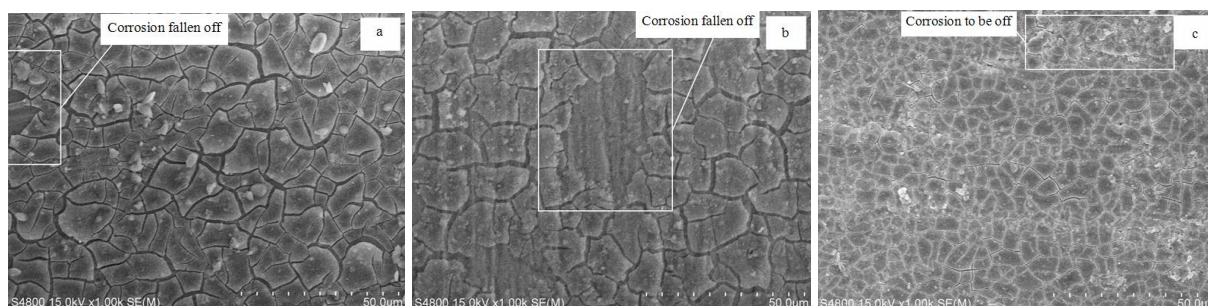
**Figure 2.** The corrosion photos of each specimen: (a) sample 1; (b) sample 2; (c) sample 3; (d) sample 4; (e) sample 5; (f) sample 6; (g) sample 7; (h) sample 8; (i) sample 9 and (j) Base metal.

Fig.3 shows SEM images of the base metal after immersion 120 h. It can be seen that the surface of base metal has been corroded completely, and exhibits some intergranular cracks. Some tiny particles peel off easily by slightly abrasion. Besides, some dip corrosion pits and loose hole can be

observed clearly in Fig.3(b). Along with the corrosion process, the corrosion will permeate from the surface to the inside of the sample. Finally, the base metal will failure due to the large area of fall off.



**Figure 3.** The SEM photos of base metal corrosion: (a) Intergranular crack enlarged view; (b) Deep corrosion diagram.



**Figure 4.** The SEM photos of each specimen under the same rotation speed and different welding speeds: (a) sample 1; (b) sample 2 and sample 3.

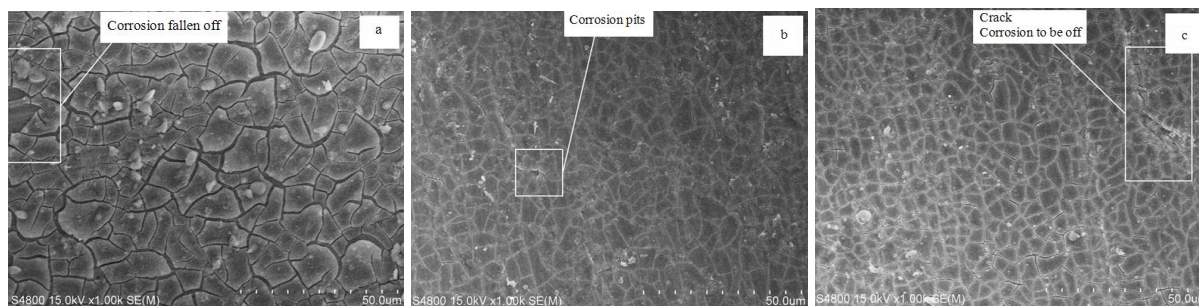


**Figure 5.** The SEM photos of each specimen under the welding speed and different rotation speeds: (a) sample 1; (b) sample 4 and sample 7.

Fig.4 displays the SEM images of corrosion surface of the sample under the rotation speed of 300 rpm and different traversing speeds. It can be seen from Fig.4(a, b) that some flaky cracks with average diameter of 10 $\mu$ m appears on the surface of the sample under long time immersion in acid solution, and different degrees of intergranular corrosion form among the flakes. In addition, the sample under the traversing speeds of 100mm/min occurs stable intergranular corrosion, and some small grains may fall off as shown in Fig.4(c). Besides that, the grain size of the sample under the traversing speeds of 100mm/min is smaller that of 30 and 50mm/min. It is mainly due to the influence

of traversing speed on the welding temperature. As the rotation speed is constant, the temperature reduces with the increasing of traversing speed, which results in smaller grain during the recrystallization process.

Fig.5 shows the SEM images of corrosion surface of the sample under the traversing speeds of 30 mm/min and different rotation speeds. As can be seen from Fig.5, the corrosion of the sample under the rotation speeds of 300rpm is the most serious. The corrosion of the sample under the rotation speeds of 600rpm has some corrosion boundary, and the surface of the sample is not crack completely. The sample under the rotation speeds of 600rpm exhibit the best corrosion resistance. There are some intergranular corrosion on the surface and smaller corrosion pits, indicating that the corrosion of sample changes from pitting corrosion to intergranular corrosion.

Fig.6 shows the weight loss of the sample immersion in different time. It can be seen that the weight losses of samples are small due to the adhesion of corrosion production. The weight losses of samples after immersion in solution for 5h become larger. Because the surface of sample is covered by corrosion oxide products, which is corroded first. And then the corrosion extends to the microstructure of welding joints. In addition, although the influence of processing parameter on the corrosion of sample obtained by the weight loss method is very small, there are still some difference in the corrosion of samples. Zhao et al. [19] had done the 6082 aluminum alloy corrosion by the immersion method. It is found that the different parameters of FSW samples of the corrosion are basic same. and corrosion degree of each FSW sample is smaller than the base metal, the corrosion quantities of each sample and base metal are less.

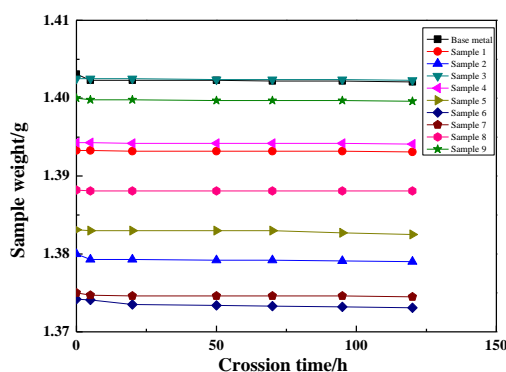


Figure 6. The curves of the weight loss of specimens in different corrosion time.

### 3.2 The electrochemical corrosion results

Fig.7 displays the polarization curve of experimental samples. It can be seen that the current density increases with increasing of the potential, suggesting that there are no passivation phenomenon in the sample. This may be due to the existence of Al element, which prevents the happening of the passivation.

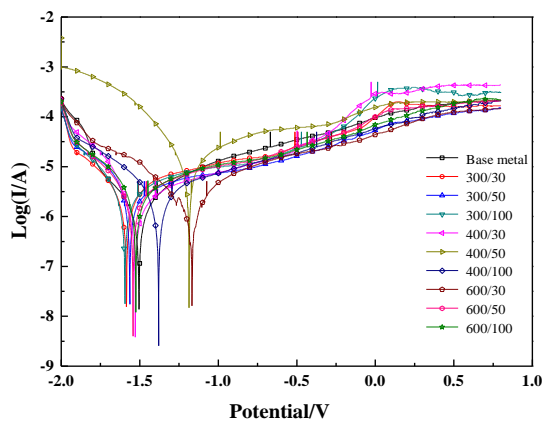
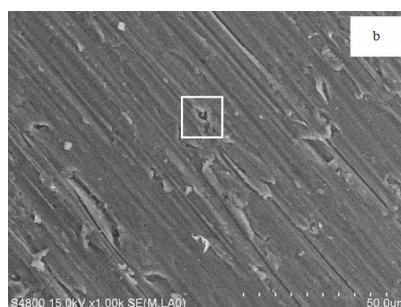
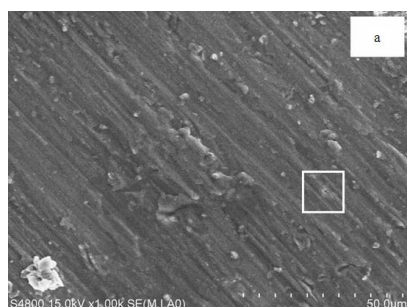


Figure 7. The polarization curve of experimental samples.

The tip of the polarization curve represents corrosion potential and corrosion current of sample, corrosion potential represents the minimum potential difference required for the happening of corrosion. The larger the corrosion potential difference means the larger corrosion potential difference needed, indicating that the happening of corrosion is more difficult. According to the electrochemical reaction mechanism, the chemical reaction rate is proportional to the current in reaction pool, so the corrosion rate is proportional to the corrosion current, suggesting that the corrosion current has great impact on the corrosion rate, and the greater the corrosion current, the larger the corrosion rate. From Table 2 can be seen corrosion potential moved negative gradually, corrosion current increased gradually, sample of the self-passivation ability is stronger. The electrochemical corrosion characteristics of 7022 aluminum alloy FSW samples are same with 5083 and LY12 aluminum alloy in Refs. [12 ] and [17]. And electrochemical corrosion properties of FSW samples are better than that of the base metal. This shows that the welding area of the grain refinement is conducive to produce the better passivation film and protect the specimen surface from corrosion.

Table 2. Each specimen of corrosion potential and corrosion current.

Sample	Base metal	1	2	3	4	5	6	7	8	9
Corrosion potential/V	-1.505	-1.607	-1.562	-1.594	-1.529	-1.184	-1.379	-1.168	-1.542	-1.525
$I \times 10^{-6}/A$	99.70	1.719	2.291	1.828	1.055	8.094	1.452	2.463	1.782	2.111



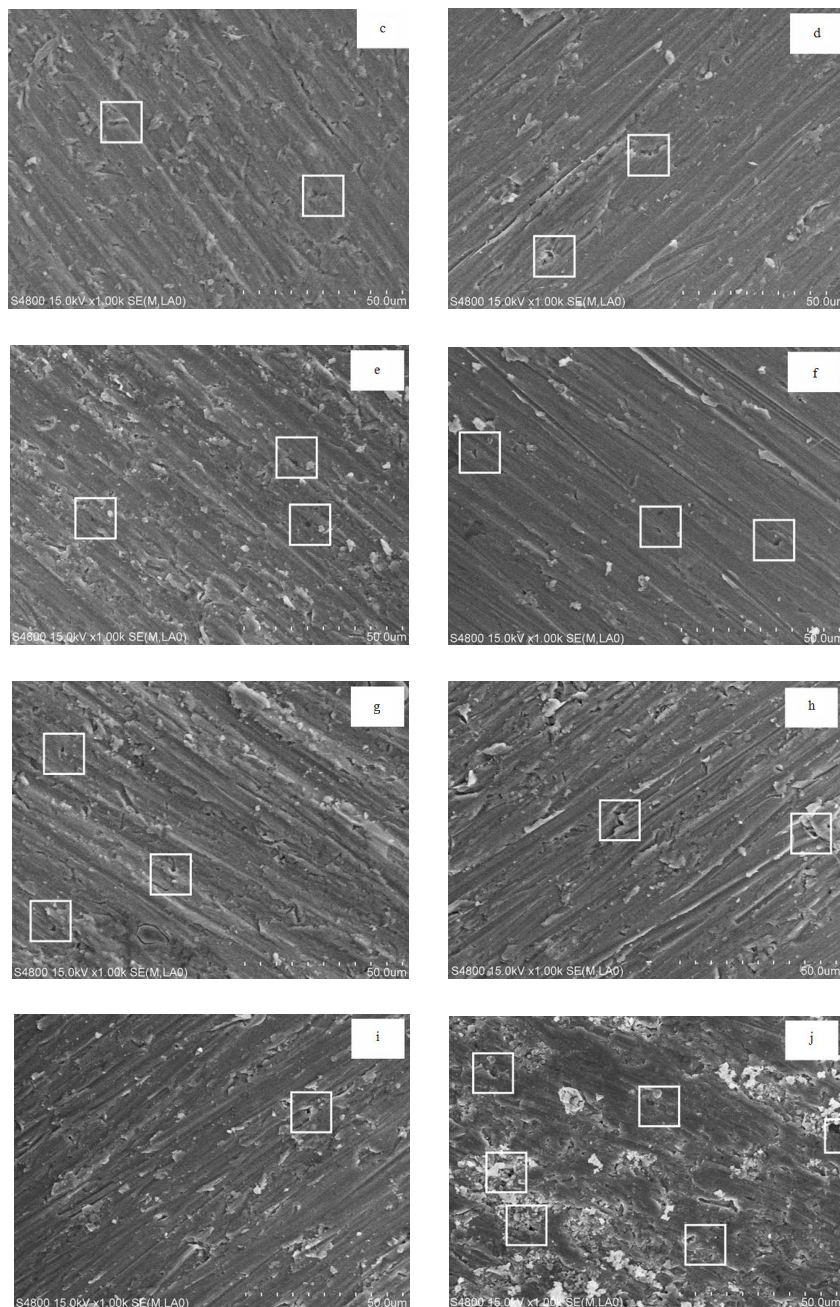


**Figure 8.** The SEM photos of each specimen of electrochemical corrosion: (a) sample 1; (b) sample 2; (c) sample 3; (d) sample 4; (e) sample 5; (f) sample 6; (g) sample 7; (h) sample 8; (i) sample 9 and (j) Base metal.

Table 2 lists the corrosion potential and corrosion current value of the parent metal and welded joints under various process parameters. It can be seen that their corrosion potential difference is small, the electrochemical corrosion performances of most welded specimens is poorer than that of the parent metal. But the electrochemical corrosion performances of the sample under 400/50, 400/100 and 400/100 are improved, indicating that the corrosion resistance can be improved by optimizing the welding process parameters, which has inconspicuous effect. It can be found from the corrosion current that corrosion rate of the base metal is far higher than those of samples under different welding parameters. The corrosion rate of sample under the process parameters of 400/30 is lowest, which is

significantly lower than those of other samples. The results are consistent with the results of weight loss. It can be concluded that the corrosion resistance of 7022 aluminum alloy can be improved observably by the friction stir welding, followed by the optimization of friction stir welding process parameters.

Fig.8 shows the SEM images of sample after electrochemical corrosion. It can be seen that the traces on the surface of the base metal are blurred, but those of welding samples remain clear. The surface of base metal is mainly covered by corrosion pitting, which shows that the corrosion rate of base metal is faster. This is mainly to the extension of grain and grain boundary during the rolled process, which reduces corrosion resistance. The severe corrosion area is marked by the white area in Fig.8(a)-(j), which(in Fig.8(a)-(i)) is less than those in the base metal(in Fig.8(j)), indicating that the corrosion resistance of welding joints is better than that of the base metal. Zhao et al. [19] reported the electrochemical corrosion behavior of FSW weld of 6062 aluminum alloy. The base metal severe corrosion pitting phenomenon was found. The welding seam only appeared a small amount of shallow corrosion pits. These conclusions are consistent with the experimental results of 7022 aluminum alloy in this paper. The corrosion resistance of FSW welding region of all aluminum alloy sheet are better than the base metal. The reason is associated with the welding region of the grain refinement that the previously mentioned. In the FSW welding region, the base metal produced a larger plastic deformation and happened the recrystallization, thus resulting in grain refinement and a reduction of dislocation density, at the same time causing welding region chemical composition homogenization. From the point of view of corrosion theory research, the chemical composition of homogenization is helpful for materials resistant to corrosion. In addition, the reduction of dislocation density can also reduce welding region defects, thus improving the welding region of the material corrosion resistance.

#### 4. CONCLUSION

(1) The results of weight loss method show that weight losses of experimental samples are smaller, but the corrosion behavior occurred on the surface of samples should not be neglected. Experimental results show that the corrosion of the base metal and welded samples under various parameters have occurred, the corrosion degree of base metal is serious, and the corrosion resistances of the welding joints is far greater than that of base metal. The welding joints under 400/30 show the minimum corrosion degree, intergranular corrosion occurred on its surface has just begun, and accompanied by the formation of corrosion pitting. The corrosion of the samples under other parameters changes from the stage of intercrystalline corrosion to the erosion stage, and some samples appear scaly denudation.

(2) The results of the electrochemical corrosion show that the corrosion potential difference of the base metal and welding joints is smaller, but the corrosion current of base metal is far greater than those of welding samples, which is consistent with the results of the weight-loss method. The corrosion performance of samples under different parameters has certain differences, and the corrosion performances of samples under 400/30 is the lowest. The electrochemical corrosion of base metal is mainly pitting corrosion, and its distribution is dense. The surface of welding samples appears a small

amount of slight corrosion pitting, indicating that the corrosion resistance of samples is better than that of the base metal.

## References

1. M.S. Khorrami, M. Kazeminezhad, A.H. Kokabi, *Mater. Sci. Eng. A*, 543 (2012) 243.
2. H.F. Wang, D.W. Zuo, M. Wang, L. Guang, C.L. Dong, *J Func. Mater.*, 41(11) (2010) 2029.
3. P. Palanivel, P.K. Mathews, N. Murugan, I. Dinaharan, *Mater. Des.*, 40 (2012) 7.
4. H.F. Wang, J.L. Wang, D.W. Zuo, X.L. Duan, M. Wang, *J Func. Mater.*, 43(10) (2012) 1327.
5. S. Rajakumar, V. Balasubramanian, *Mater. Des.*, 40 (2012) 17.
6. D.F. Metz, M.E. Barkey, *Int. J Fatigue*, 43 (2012) 178.
7. J. Guo, P. Gougeon, X.G. Chen, *Mater. Sci. Eng. A*, 553 (2012) 149.
8. Y.G. Yan, L. Ma, H.J. Zeng, H.B. Zhang, *Cor. Sci. Prot. Technol.*, 21 (2009) 120.
9. D. Zhang, W.H. Chen, C.G. Wang, F.B. Dong, *Cor. Prot.*, 33(2012)705.
10. L. Lu, W. Xue, X. Jin, J. Du, M. Hua, *Rare. Metal. Mater. Eng.*, 41(9) (2012) 1597.
11. S.D. Ji, L.G. Zhang, Z.L. Liu, S.S. Gao., *Hot Wor. Technol.*, 40(2011)10.
12. B.H. Hu, L. Xing, S.L. Wang, *J Nanchang Hangkong Univ.(Natl. Sci.)*, 26(2012)52.
13. C.L. Dong, C.B. Shen, Z.Z. Wang, *J Dalian Jiaotong Univ.*, 30(2009)42.
14. J. Kang, S.Y. Liang, G. Li, G.H. Luan, C.L. Dong, M. He, R.D. Fu, *Cor. Sci. Prot. Technol.*, 24(2012) 51.
15. K. Sureha, B.S Murty, R.K Prasad, *Surf. Coat. Technol.*, 202 (2008) 4057.
16. H. Omar, *Mater. Sci. Eng. A*, 492 (2008) 168.
17. Y.D. Zhao, C.B. Shen, S.H. Liu, J.P. Ge, Z.H. Huang, C.L. Dong, *J Dalian Jiaotong Univ.*, 29(2008)68.
18. C.B. Shen, Y.D. Zhao, S.H. Liu, J.P. Ge, Z.H. Huang, C.L. Dong, *J Aeron. Mater.*, 29(2009)24.
19. Y.D. Zhao, C.B. Shen, S.H. Liu, J.P. Ge, Z.H. Huang, *Tran. Chin. Weld Inst.*, 29(2008)105.

© 2016 The Authors. Published by ESG ([www.electrochemsci.org](http://www.electrochemsci.org)). This article is an open access article distributed under the terms and conditions of the Creative Commons Attribution license (<http://creativecommons.org/licenses/by/4.0/>).